TECHNICAL RESEARCH REPORT

Comparison of Responses in the Anterior and Primary Auditory Fields of the Ferret Cortex

by N. Kowalski, H. Versnel and S.A. Shamma

T.R. 94-51

Sponsored by
the National Science Foundation
Engineering Research Center Program,
the University of Maryland,
Harvard University,
and Industry

Comparison of Responses in the Anterior and Primary Auditory Fields of the Ferret Cortex

Nina Kowalski[a], Huib Versnel[b] and Shihab A. Shamma[a]

(a) Electrical Engineering Department and Institute for Systems Research, University of Maryland, College Park, MD 20742.

(b) Institute for Systems Research, University of Maryland, College Park, MD 20742.

ABSTRACT

Characteristics of an anterior auditory field (AAF) in the ferret auditory cortex are described in terms of its electrophysiological responses to tonal stimuli and compared to those of primary auditory cortex (AI). Units in both areas were presented with the same stimulus paradigms and their responses analyzed in the same manner so that a direct comparison of responses was possible. The AAF is located dorsal and rostral to AI on the ectosylvian gyrus and extends into the suprasylvian sulcus rostral to AI. The tonotopicity is organized with high frequencies at the top of the sulcus bordering the high-frequency area of AI, then reversing with lower BFs extending down into the sulcus. AAF contained single units that responded to a frequency range of 0.2 - 30 kHz. Stimuli consisted of single-tone bursts, two-tone bursts and frequency modulated (FM) stimuli swept in both directions at various rates. Best frequency (BF) range, rate-level functions at BF, directional sensitivity, and variation in asymmetries of response areas were all comparable characteristics between AAF and AI. The characteristics that were different between the two cortical areas were: latency to tone onset, excitatory bandwidth 20 dB above threshold (BW20) and preferred FM rate, as parameterized with the centroid (a weighted average of spike counts). The mean latency of AAF units was shorter than in AI (16.5 ms AAF, 19.4 ms AI). BW20 measurements in AAF were typically twice as large as those found in AI (2.5 oct AAF, 1.3 oct AI). There was a wider range of centroids found in AI than in AAF, and the relationships between BW20 and centroid were different for AAF and AI. The relationship between centroid and BW20 was examined to see if wider bandwidths were a factor in a unit's ability to detect fast sweeps. There was significant ($P<0.05$) linear correlation in AAF but not in AI. In both fields, the variance of the centroid population decreased with increasing BW20. BW20 decreased as BF increased for units in both auditory fields.

INTRODUCTION

An auditory cortical field is defined physiologically as a region in the auditory cortex containing neurons that are selectively sensitive to auditory stimuli for a contiguous, tonotopically ordered frequency range (Merzenich and Schreiner 1992). Besides the primary auditory field (AI), other auditory fields have been mapped in the mammalian auditory cortex, including the anterior auditory field (AAF) (Tunturi 1962; Merzenich and Brugge 1973; Knight 1977; Redies et al. 1989), and auditory fields rostral or rostralventral to AI (Suga 1965; Merzenich and Brugge 1973; Aitkin et al. 1986; Redies et al. 1989; for comprehensive review see Merzenich and Schreiner 1992). In addition, non-tonotopic auditory areas, including the secondary auditory cortex of the cat (AII) have been described (Schreiner and Cynader 1984). The presence of more than one tonotopically ordered auditory area has led to the suggestion that they might provide explicit representations of various perceptually significant features in the acoustic stimulus. This parcelization has close parallels in other sensory systems such as the visual and somatosensory cortex (Kaas et al. 1981; Zeki and Shipp 1988). In the visual cortex, electrophysiological, behavioral, and anatomical experiments have all largely confirmed that processing of different aspects of an image (e.g., form, color, or motion), tend to be concentrated in distinct cortical fields (V2- V5), with the primary field (VI) serving as the gateway to all other fields (DeYoe and Van Essen 1988; Zeki and Shipp 1988).

In the auditory cortex, anatomical studies have uncovered many complex forward-, backward- and inter-connections among its different subdivisions (Mastubara and Phillips 1989; Winer 1992). Furthermore, many electrophysiological investigations have described distinct overall response characteristics among the various auditory cortical subdivisions (Clarey et al. 1992). Therefore, it is possible that the auditory cortex is functionally organized in the same segregated manner as visual cortex. To explore this possibility, it is necessary to characterize in detail the response properties of the different auditory fields to various stimulus manipulations. So far, AI has been the only extensively studied area in the auditory cortex (Merzenich and Schreiner 1992). In this paper, we describe in detail the electrophysiological responses of AAF in the ferret (*Mustela putorius*), and compare them to those found in AI.

Unlike the cat, there has not been anatomical information about the thalamo-cortical connectivity of these areas for the ferret until very recently. The results of Angelucci et al. (1993) reveal that a cortical area rostral to AI receives a major portion of its afferent connections from the medial portion of the medical geniculate body (MGB), while the AI receives most of its afferent connections from the ventral portion of the MGB. However, because there is substantial overlap in these projections, it is not completely clear whether these can be considered distinct 'parallel' pathways to the auditory cortex originating from functionally separate areas of the MGB.

In addition to general response characteristics such as latency to tone onset, two types of response properties will be discussed in this report: (1) those summarizing the shape of the response area of the cells such as threshold and the best frequency (BF) of a cell, the asymmetry of its inhibitory and excitatory responses about the BF, and the bandwidth of its excitatory field; (2) and those associated with responses to frequency-modulated (FM) tone stimuli, such as the sensitivity of a cell's response to the direction and rate of FM sweeps. Previous experiments in the ferret (Kelly et al. 1986a; Philips et al. 1988; Shamma et al. 1993; Shamma et al. 1994; Versnel et al. 1994) have described in detail some of these response characteristics in AI cells. For example, in the ferret AI, Shamma et al. (1993) report a correspondence between a unit's response area asymmetry and its selectivity to the direction to FM stimuli. We examine whether this relationship between response area asymmetry and FM directional sensitivity is also found in ferret AAF. In addition, since preliminary measurements indicate that ferret AAF units have a wider range of bandwidths than those in AI, we test for selectivity to FM rates to see if excitatory bandwidth plays a role in the rate-detection mechanism (Kowalski et al. 1993; Wang and Shamma 1994; Heil

et al. 1992a; Mendelson et al. 1993). These studies in the ferret are supported or complemented by several studies in the cat (Reale and Imig 1980; Mendelson and Cynader 1985; Phillips et al. 1985; Schreiner and Mendelson 1990; Schreiner and Sutter 1992; Heil et al. 1992b, c; Mendelson et al. 1993). The experimental paradigms and response measures are applied here to the ferret AAF so as to compare directly its responses to those of AI.

METHODS

Surgery and Animal Preparation

The techniques involved in the surgery and preparation for data recording are described in detail in Shamma et al. (1993). The data were collected from a total of 24 ferrets, 7 for AAF and 17 for AI, each weighing between 1.0 - 1.8 kg. A portion of the AI data were used in another study (Shamma et al. 1994). The ferrets were anesthesized with pentobarbital sodium (40 mg/kg ip) and maintained in an areflexic state during the entire experiment using a continuous intravenous infusion of pentobarbital (5 mg/kg/hr) diluted with dextrose-electrolyte solution. The ectosylvian gyrus containing AI (Kelly et al. 1986a; Kavanagh and Kelly 1987) and the suprasylvian sulcus, where the AAF is found, were exposed by craniotomy. The dura was incised and reflected, and the surface of the brain covered with agar to reduce pulsations. A Sony MDR-E464 miniature speaker was attached to a speculum sewn on to the exposed meatus. Data collection typically lasted 24 - 30 hours following the surgery and preparation.

Acoustic Stimuli

Pure tone stimuli (single- and two-tone bursts, 200 ms duration, 10 ms rise and fall times, 50 ms intertone delay) were generated using two independent function generators, gated and mixed, and then fed through a common equalizer into the earphone. FM sounds (10 ms rise-fall times, 500 ms duration) were generated by a single function generator and consisted of tones swept logarithmically 2-3 octaves about the BF, in both directions, at various modulation rates. Modulation rates varied between 30 - 300 octaves/s in steps of 30 octaves/s. Calibration of the sound delivery system (≤20kHz) was performed in situ before each experiment using a 1/8-inch Brüel & Kjaer probe microphone (type 4170) and an automated calibration setup as described in Shamma et al. (1993). The calibration was assumed to be unreliable at very high frequencies (>26kHz), therefore units with very high-frequency responses were excluded from the data analysis.

Recording Procedures

Single-unit action potentials were recorded using glass-insulated tungsten microelectrodes with 5 to 6 MΩ impedances. The recorded signals were led through amplifiers (x10,000) and filters (0.5 - 5 kHz BP). Single units were isolated and identified through manual adjustment of a windowing amplifier. A consistent spike waveform shape differentiated the single unit recordings from the cluster recordings. The time of spike occurrence relative to stimulus delivery was stored using a Hewlett-Packard 9000/800 series minicomputer. The computer also controlled stimulus delivery and created raster displays and spike count histograms of the responses. In each paradigm, a stimulus is presented every second, and the sampling rate is 5 kHz.

In AI, electrode penetrations were made orthogonally to the cortical surface. Recordings were typically made at depths of 300 - 600 μm, corresponding to cortical layers III and IV (Shamma et al. 1993). In AAF, electrode penetrations were made parallel to the depth of the suprasylvian sulcus, approximately 0.5 mm caudal of the sulcus so that cortical layers III and/or IV were reached. Figure 1 shows a schematic of electrode penetrations in AAF. Each penetration in the AAF consisted of units at depths ranging from 400 - 3000 μm.

Data Analysis

The following characteristics were measured from each cortical unit: best frequency (BF), latency, threshold, rate-level function, response area curve, inhibition asymmetry index (M), FM directional sensitivity index (C), and FM rate index (centroid). BF is defined as the frequency of the lowest threshold and is verified for each cell with a response plot performed at up to 1/6 octave resolution at low intensity. The other parameters were all measured from three types of raster plots generated for each single unit: rate-level, two-tone, and FM sweep. The rate-level plot is the collection of responses to a tone at BF at varying intensities, typically a range of 35 - 85 dB SPL in steps of 10 dB. This test is used to measure the best intensity, threshold and latency to tone onset of a single unit. A cell was defined nonmonotonic if its rate-level curve at higher intensities decreased by more than 25% of total spike count, and its best intensity the intensity of maximum response. The threshold is the intensity at which the spike count reached 10% of the maximum. Latency is measured to be the period between the onset of the stimulus and the time corresponding to the maximum of a post-stimulus time histogram with a bin width of 1 or 2 ms. For each unit, the shortest latency over a range of intensities (35 - 85 dB SPL, 10 dB steps) was measured and included in the data analysis.

The response area of a unit is determined from the two-tone stimuli paradigm, where two tone bursts of equal duration with onset times staggered by 25 or 50 ms are presented (see Shamma et al. 1993 for details). The first tone (T1) varied in frequency about the BF and is used to explicity measure the excitatory portion of the response area. The second tone (T2) is only presented at the best frequency, at an intensity that produces a strong response; it is used to provide a level of background activity against which the inhibitory response area can be measured. This elevation of activity was necessary because many cells exhibited low firing rates, partly because of the depression of spontaneous activity by the anesthetic used in these experiments (Brugge and Merzenich 1973; Pfingst and O'Connor 1981). Figure 2 depicts the two-tone paradigm graphically.

The response area is constructed from the collection of two-tone tests perfomed at various T1 intensities. A measure of asymmetry in the excitatory and inhibitory portions of the response area was introduced in Shamma et al. (1993):

$$M = \frac{R_{>BF} - R_{<BF}}{R_{>BF} + R_{<BF}}$$

where $R_{>BF}$ and $R_{<BF}$ are the total number of spikes to both tones for an equal number of frequencies above and below the BF, respectively. If the excitatory and inhibitory responses are approximately symmetric around BF, the measure M will be near zero. Inhibition of T2 responses by T1 stimuli above BF and/or spread of the response to T1 towards lower frequencies (<BF) causes M to be negative. Conversely, stronger low frequency inhibition or high frequency T1 excitation produces positive M values. Figure 2 shows examples of the three types of M indices that are measured: positive, near zero, and negative. A response area is made up of two-tone tests performed over a range of intensities. An M index that describes a response area is the average M index over all intensities. Excitatory bandwidth is measured from the response area curve. The bandwidth measure, BW20, is the number of octaves over which an excitatory response exists at 20 dB above threshold. The 20 dB figure was chosen based on the observation that most units did not saturate at 20 dB above threshold according to their rate-intensity curves. The upper and lower frequencies were found by interpolation using a criterium of 10% of the maximum response. Spontaneous activity was measured and subtracted from the total spike counts before bandwidth measurement.

Figure 3 shows a raster plot of a FM response and corresponding stimulus parameters. A unit's directional sensitivity to the two sweep directions is assessed using the index C as follows

$$C = \frac{R\downarrow - R\uparrow}{R\downarrow + R\uparrow}$$

where $R\downarrow$and $R\uparrow$ are the spike counts due to the up and down sweeps, respectively. Thus, if the C index is close to zero, the cell does not display selectivity to one direction over another. If the C index is more negative, then the cell is selective to upsweeps and vice-versa for positive C values. The centroid parameter is used to describe FM rate selectivity of a cell. The centroid is an average of the stimuli rates, weighted by the number of responses at each rate. In estimation theory, the centroid is also known as the minimum-mean square error estimator (MMSEE) (Poor 1988):

$$E\{X|\theta\} = \sum_{x=30}^{x=300} xp(x|\theta)$$

where the preferred rate of a cell is modeled as the random variable X and its distribution given the observations is the response amplitude curve generated from the spike counts at each rate. Thus, the centroid is also measured in octaves/s and is simply an estimator of the preferred rate given the measured responses. For comparison purposes, another measure of preferred rate was examined, namely the rate of maximum spike count. The rate of maximum spike count was computed from the same raster plots used to compute the centroid measure. Total spike counts were calculated for each rate over the time window corresponding to the upsweep or downsweep, whichever sweep induced the most spikes. The rate corresponding to the largest total spike count was chosen.

An unpaired Student's t-test and the F-test for variance are performed for each characteristic examined in the AAF and AI. These tests are performed to determine the likelihood of the observed difference occurring by chance.

RESULTS

Data presented here are from 89 single units found in AAF of 7 ferrets and from 169 single units found in AI of 17 ferrets. We attempted to perform all test paradigms (see *Methods*) for each single unit; in some cases the length of time a single unit remained isolated was limited.

Location

The AAF is located on the ectosylvian gyrus and extends into the suprasylvian sulcus rostral to the primary field as shown in Fig. 4. The tonotopicity is organized with high frequencies at the top of the sulcus bordering the high-frequency area of AI, then reversing with lower BFs extending down into the sulcus. Figure 5 shows the variation in BF with depth for two animals. Long penetrations (3000 μm) into the suprasylvian sulcus at depth intervals of 100 μm revealed orderly decreases in BF for all animals. It is likely we made our recording tracks approximately perpendicular to, or at some angle to the isofrequency lines.

General response characteristics

The AAF contained single units that had BFs in the frequency range 0.3 - 30 kHz. AI units had a BF range of 0.6 - 12 kHz. Units with higher-frequency BFs (>14kHz)were observed, but not analyzed due to calibration limitations (see *Methods*). The distribution of BFs is shown in Fig. 6. Units with this range of BFs are found in AAF and AI in similar proportions.

The time course of responses is described by latency to onset of single tones, and whether the response is phasic or sustained. Units in AAF are phasic, as is the case in AI. This may be related to the fact that all animals were maintained at similar levels of anesthesia. Figure 7 shows the distributions of latencies in each field. A comparison of means test showed that the AAF mean latency (16.5 ms) was significantly shorter than the AI mean latency (19.4ms) ($P<0.0001$).

Figure 8 describes the distribution of rate-level functions in both populations. The distributions of monotonic units to non-monotonic units in AAF and AI are not significantly different ($P>0.05$; 45% non-monotonic in AAF, 58% non-monotonic in AI). Figure 9 shows the distributions of tonal thresholds at BF in the AAF and AI. The data show that mean thresholds (47 dB SPL in AAF, 49 dB SPL in AI) are very similar among the two auditory fields.

Response areas, asymmetries and bandwidths

AAF units have response areas comparable to those of AI units. Response areas of units from both cortical areas vary in shape and detail, but can generally be grouped into three categories by the asymmetry of their inhibitory sidebands. Response areas were either symmetric (type I), or asymmetric (types II and III) depending on the locations of the excitatory and inhibitory areas about the best frequency. Examples of response areas from units in both AI and AAF are shown in Fig. 10.

The most pronounced difference between AI and AAF response areas is that the excitatory bandwidths of the AAF response areas are significantly wider than those of AI. Figure 11A shows the distribution of BWs in AAF and AI, respectively. The mean BW20 in AAF (2.5 octaves) is approximately twice as large as the mean BW20 in AI (1.3 octaves). Their difference is statistically significant ($P<0.0001$). Bandwidths are correlated to BF for both AAF and AI. This relationship is shown in Fig. 11B. In both cases, BW20 tends to decrease as best frequency increases. In AAF, the trend seen for BW20 vs. BF seems to be directly proportional to that of AI. The slope of a regression

line used to fit the data is translated by approximately a factor of 2 for AAF as compared to AI.

The distribution of *M* indices is used to quantitatively describe the distribution of the response area types found in each field. Figure 12 shows the distribution of *M* indices in each cortical area. The populations are not statistically different ($P>0.05$), indicating that there are similar proportions of response area asymmetry types in AAF and AI.

FM directional sensitivity

Like AI units, AAF units also show FM directional sensitivity as measured with the *C* index. The distributions of *C* indices for AAF and AI were comparable (Figure 13). As is the case in AI, the unit's response area asymmetry (type I, II or III) is correlated with the direction to which the unit is most sensitive. Cells with type I response areas (symmetric) respond equally well to upward and downward sweeps. Cells with type II response areas (inhibition above the BF) and type III response areas (inhibition below the BF) respond best to upward and downward sweeps, respectively. Figure 14 shows the population of *M* indices plotted against the *C* indices for AI and AAF. There is a significant correlation in both fields ($P<0.05$) between a cell's response area symmetry and its directional selectivity.

FM rate sensitivity

A narrower range of centroids was found in AAF than in AI (Figure 15A). The variance of the AAF centroid population (SD=27) was significantly smaller than in AI (SD=34) ($P<0.05$, F-test). The range of centroids found in AI was 50-250 oct/s whereas the centroids found in AAF were between 100-200 oct/s. On the other hand, the mean centroids (159 oct/s in AAF, 157 oct/s in AI) were not significantly different. Scatterplots of centroid versus BW20 are shown in Fig. 15B. Centroid and BW20 were significantly correlated for AAF units ($P<0.05$), but not for those in AI ($P>0.05$). Figure 15B also shows the following for both AI and AAF: the lower bound of the centroid range increases as BW20 increases, as shown by the dotted line connecting the mean -2SD points. The mean +2SD bound (upper bound) remains constant or decreases within each field. This relationship can also be described by a decrease in centroid variance for wider BW20. Centroid variances are comparable between AAF and AI for BW20 below 2 octaves; above 2 octaves, the centroid variance is smaller for AAF than in AI.

In order to examine any effect of the different rate-level functions among units, the units were divided into monotonic and non-monotonic groups. Both groups showed the same trends of centroid vs. BW20 as seen for the entire population. We also examined the effect of using another measure of preferred rate, the rate of maximum spike count, instead of the centroid. There was more scatter in the rate of maximum spike count measure compared to the centroid. However, BW20 was also correlated to rate of maximum spike count in AAF (R=0.38) and not in AI (R=0.04), so the differences between measures did not significantly affect our results.

DISCUSSION

Similarities and differences between AI and AAF

The results of this comparative study are summarized in Table 1. In comparisons other than for BF range, the difference was determined to be significant if either a t-test for means or a F-test for variance showed that the populations statistically differed ($P<0.05$). BF range, rate-level functions at BF, directional sensitivity, and variation in asymmetries of response areas were all comparable characteristics between AAF and AI. This suggests that single unit tonal response curves, including the variability about BF in excitation/inhibition asymmetries, are the same for AI and AAF. In other words, the tonal response of an AAF unit can be described in the same manner as one in AI, namely, with response areas at varying intensities, or an excitatory/inhibitory tuning curve. Also, as previously found in ferret AI (Shamma et al. 1993), there was a correspondence between the *M* index (describing response area asymmetry) and the *C* index (describing FM directional sensitivity). This supports the idea (Heil et al. 1992a; Shamma et al. 1993) that a unit's response area asymmetry is a determining factor in its sensitivity to a given sweep direction. The major differences between the two cortical areas were: latency, excitatory bandwidth and the preferred FM rate (centroid) of single units.

Comparison of latencies between AI and AAF

The observed difference in mean latencies may reflect the connectivity with underlying auditory areas. The latencies reported could mean that AAF receives thalamic input before AI, but the lack of information on thalamo-cortical and intra-cortical area connectivity precludes us from knowing whether the order is relevant. It might be that both areas receive information in parallel, and the latency is due to the respective conduction time from the MGB. The results in the ferret by Angelucci et al. (1993) state that a cortical area in the ventral suprasylvian sulcus receives most of its afferent connections from the medial portion of the medial geniculate body (MGB), while the AI receives most of its afferent connections from the ventral portion of the MGB. However, because this area may not correspond to AAF and because there is substantial overlap in these projections, it is not clear whether there are 'parallel' pathways to the auditory cortex originating from functionally separate areas of the MGB, or if the differences between the two auditory fields are cortical in origin. Anatomical studies in the cat auditory cortex report that AAF and AI receive similar thalamic input (Anderson et al. 1980) and electrophysiological studies report that latencies between AAF and AI are comparable (Knight 1977; Phillips and Irvine 1982). Morel and Imig (1989) report that AAF in the cat receives a substantial input from a subdivision of the MGB called Po, the lateral part of the posterior group of thalamic nuclei. Like the ventral MGB, this area typically contains neurons with short latencies (Phillips and Irvine 1989). More anatomical information, especially in the ferret, is required before thalamocortical comparisons can be made with the cat. It should be noted that the ferret auditory system is similar to the cat's system in physiology. Differences are that the ferret ear is less sensitive and is shifted towards lower frequencies (Kelly et al. 1986b).

Comparison of excitatory bandwidths between AI and AAF

The most pronounced difference between AAF and AI is that a unit in AAF is better represented with wider excitatory tuning curves. The distribution of BW20 in AAF is shifted towards higher values relative to the BW20 distribution in AI (Fig. 11A). In effect, the AAF bandwidth range can be looked at as increasing the range of bandwidths in AI. Including AAF bandwidths adds to the effective bandwidth range across all BFs in the cortex (Fig. 11B).

Unlike our results in the ferret, excitatory bandwidths in cat AI are comparable to excitatory bandwidths in cat AAF. Two reports on cat AAF physiology (Phillips and Irvine 1982; Knight 1977) state that AAF and AI cells were very similar in characteristics such as: tuning, intensity functions, response latencies. Examinations of thalamic connections to AI and AAF in the cat (Andersen et al. 1980; Morel and Imig 1987) have concluded that AI shows more connectivity with the ventral MGB, and AAF contains denser projections from the magnocellular and deep dorsal MGB but with also significant input from ventral MGB. The connectivity is relevant because it has been shown that in the cat, the ventral MGB shows tonotopic organization and sharp frequency tuning whereas the magnocellular and deep dorsal MGB shows no tonotopic organization and has wider breadth of tuning (Aitkin 1973; Toros-Morel et al. 1981; Calford 1983). Whether the ferret AAF neurons have wider excitatory bandwidths due to its thalamocortical connections or whether the wider bandwidths are generated cortically remains to be investigated.

The functional significance of wider bandwidths may be to detect broad features of a spectral profile (Calhoun and Schreiner 1993; Shamma et al. 1994; Wang and Shamma 1994). Wide response areas are better matched to broader spectral modulations of a stimulus. Another function may be that wider bandwidths play a role in the detection of stimuli that are rapidly changing in time. Assuming temporal integration of auditory input, fast FM sweeps correspond to broad stationary spectrums.

Comparison of rate selectivity between AI and AAF

Rate selectivity, as measured by the centroid, differed between AAF and AI in two ways: 1. the distribution of centroids was significantly different between fields and 2. the relationship between centroid and excitatory bandwidth was different for AI than for AAF. The range of AAF centroids fell entirely within the range of AI centroids (Fig. 15A); in fact, based on centroid distribution alone, AI units would be better suited for implementing rate selectivity, simply due to its ability to detect a wide range of centroids. It is apparent that AAF does not serve the purpose of selectively detecting rapid FM rates.

There was significant correlation between centroid and excitatory bandwidth in the AAF. In contrast, there was no correlation between centroid and excitatory bandwidth in AI. There was, however, a relationship between centroid and excitatory bandwidth in both fields that is best described as triangular (dashed lines in Fig. 15B). As bandwidth increases, the corresponding centroid population decreases in variance. Heil et al. (1992a) also found a relationship similar to this one in the chick and describes the centroid ranges as having an increasing "lower bound" as bandwidth increases. However, there are discrepancies in the literature: a correlation between FM rate and bandwidth in cat AI was found by Mendelson et al. (1993) but not by Heil et al. (1992b) (the latter thus agreeing with ferret AI). There were differences between the studies including the species, FM sweep stimuli and data analysis methods, but it is not clear whether they could have affected the results. For instance, using linear (Heil et al.) instead of logarithmic sweeps (Mendelson et al.; this paper) does not significantly affect the estimate of the rate sensitivity (Versnel and Nelken 1994), and when our data were analyzed with a measure of preferred rate similar to Heil et al., the outcome did not change.

The differences in FM-rate-vs.-bandwidth relationships between the two fields imply that excitatory bandwidth is not the primary feature involved in the rate detection mechanism in the ferret. Excitatory bandwidth can play a limited role in the process as shown by the significant correlation in AAF. Another characteristic that might be involved in rate selectivity and that is not correlated with the excitatory bandwidth is sideband inhibition. Since response area inhibition asymmetry has been shown to correlate with FM directional sensitivity (as discussed above), it is reasonable to hypothesize that inhibitory sidebands may also be involved in other aspects of the FM response. For instance, units with various inhibitory bandwidths, various asymmetries about BF and the same excitatory bandwidths (cf. Fig. 10) may respond differently since the FM stimulus passes through both inhibitory and excitatory areas. Unfortunately, it is hard to analyze the effect of inhibition since, e.g., estimates of inhibitory measures depend on the second tone in the two-tone test (see METHODS). To summarize, our results imply that the width of excitatory area is not the sole factor determining a unit's rate sensitivity. The variable we are measuring is most likely only one of those involved in the complete mechanism.

Hypothesis on the generation of wider response areas

In the visual cortex, the function of wide receptive fields is thought to be essential to the processing of whole scenes, where the information in many smaller fields of view must be compared with each other. Larger receptive fields may be generated through topical convergence or confluent convergence (Zeki and Shipp 1988). Topical convergence occurs when the projecting area is larger then the area projected to, for example, the projection of many blobs in V1 to a thin stripe in V2 (Livingstone and Hubel 1984). Confluent convergence describes the integration across functionally separate areas. In the auditory cortex, AAF might be considered the result of topical convergence of thalamic pathways, but probably not the result of confluent convergence of AI pathways, since latencies to tones are comparable or shorter in AAF. If AAF is smaller in area than AI, and if one assumes that the projections to AAF and AI from MGB are approximately equal, then perhaps wider response areas are being generated through topical convergence. We hypothesize that the convergence of many excitatory connections, each of a small range of frequency results in a effective widening of the frequency response of a cell. Contiguous excitatory connections may be formed, resulting in a wide continuous excitatory response. Figure 16 shows a schematic of the hypothesized neural connectivity. In this configuration, temporal summation of EPSPs evoked by an FM sweep is optimal for a certain FM rate (Heil et al. 1992a). It is conceivable that a large number of connections is required per neuron (such as in AAF but not in AI) in order for temporal summation to contribute significantly to rate detection selectivity. Another yet unknown mechanism such as inhibition or is thought to be responsible for rate selectivity in AI.

In summary, AAF and AI contain units that can be described with similar parameters, but with variation in the range of these parameters. Significant differences that we described in our data between the two fields are: shorter latencies, larger excitatory bandwidths and FM rate sensitivity characteristics. However, before a functional significance can be ascribed to this finding, it is essential first that an explicit and realistic model of FM rate sensitivity be formulated and tested in both cortical fields.

ACKNOWLEDGMENTS

We thank P. Gopalaswamy for help in developing the data acquisition system, and A. Owens and P. Wiser for assistance in data recordings.

This work is supported in part by grants from the Air Force Office of Scientific Research, and the Office of Naval Research. The authors are members of the Institute for Systems Research, which is partially funded by a National Science Foundation Grant (NSFD CD-8803012).

REFERENCES

AITKIN, L. M. Medial geniculate body of the cat: responses to tonal stimuli of neurons in medial division. *J. Neurophysiol.* 36: 275-283, 1973.

AITKIN, L. M., IRVINE, D. R. F., NELSON, J. E., MERZENICH, M. M. AND CLAREY, J. C. Frequency representation in the auditory midbrain and forebrain of a marsupial, the northern native cat (Dasyurus hallucatus). *Brain Behav. Evol.* 29: 17-28, 1986.

ANDERSEN, R. A., KNIGHT, P. L. AND MERZENICH, M. M. The thalamocortical and corticothalamic connections of AI, AII and the anterior auditory field (AAF) in the cat: Evidence for two largely segregated systems of connections. *J. Comp. Neurol.* 194: 663-701, 1980.

ANGELUCCI, A., CLASCÁ , F. AND SUR, M. Multiple cortical auditory fields in the ferret defined by their architectonics and thalamocortical connections. *Soc. Neurosci. Abstr.* 19: 1427, 1993.

BRUGGE, J. F. AND MERZENICH, M. M. Responses of neurons in auditory cortex of the Macaque monkey to monaural and binaural stimulation. *J. Neurophysiol.* 36: 1138-1158, 1973.

CALFORD, M. B. The parcellation of the medial geniculate body of the cat defined by the auditory response properties of single units. *J. Neurosci.* 3: 2350-2364, 1983.

CALHOUN, B. M. AND SCHREINER, C. E. Spatial frequency filters in cat auditory cortex. *Soc. Neurosci. Abstr.* 19: 1422, 1993.

CLAREY, J. C., BARONE, P. AND IMIG, T. J. Physiology of Thalamus and Cortex. In: *The Mammalian Auditory Pathway: Neurophysiology* edited by A. N. Popper and R. R. Fay. New York: Springer-Verlag, 1992, p. 232-334.

DEYOE, E. A. AND VAN ESSEN, D. C. Concurrent processing streams in monkey visual cortex. *Trends Neurosci.* 11: 219-226, 1988.

HEIL, P., LANGNER, G. AND SCHEICH, H. Processing of frequency-modulated stimuli in the chick auditory cortex analogue: evidence for topographic representations and possible mechanisms of rate and directional sensitivity. *J. Comp. Physiol. A.* 171: 583-600, 1992a.

HEIL, P., RAJAN, R. AND IRVINE, D. Sensitivity of neurons in cat primary auditory cortex to tones and frequency-modulated stimuli. I: Effects of variation of stimulus parameters. *Hear. Res.* 63: 108-134, 1992b.

HEIL, P., RAJAN, R. AND IRVINE, D. Sensitivity of neurons in cat primary auditory cortex to tones and frequency-modulated stimuli. II: Organization of response properties along the 'isofrequency' dimension. *Hear. Res.* 63: 135-156, 1992c.

KAAS, J. H., SUR, M., NELSON, R. J. AND MERZENICH, M. M. The postcentral somatosensory cortex. Multiple representations of the body in primates. In: *Cortical Sensory Organization* edited by C. N. Woolsey. Clifton, NJ: Humana Press, 1981, p. 29-45.

KAVANAGH, G. L. AND KELLY, J. B. Contribution of auditory cortex to sound localization by ferret Mustela putorius. *Hear. Res.* 24: 111-115, 1987.

KELLY, J. B., JUDGE, P. W. AND PHILLIPS, D. P. Representation of the cochlea in primary auditory cortex of the ferret *Mustela putorius*. *Hear. Res.* 9: 35-41, 1986a.

KELLY, J. B., KAVANAGH, G. L. AND DALTON, J. C. H. Hearing in the ferret *(Mustela putorius)*: thresholds for pure tone detection. *Hear. Res.* 269-275, 1986b.

KNIGHT, P. L. Representation of the cochlea within the anterior auditory field (AAF) of the cat. *Brain Res.* 130: 447-467, 1977.

KOWALSKI, N., VERSNEL, H. AND SHAMMA, S. A. Characteristics of an anterior auditory field in the ferret auditory cortex. *Assoc. Res. Otolaryngol. Abstr.* 16: 130, 1993.

LIVINGSTONE, M. S. AND HUBEL, D. H. Anatomy and physiology of a color system in the primate visual cortex. *J. Neurosci.* 4: 309-356, 1984.

MATSUBARA, J. A. AND PHILLIPS, D. P. Intracortical connections and their physiological correlates in the Primary auditory cortex (AI) of the cat. *J. Comp. Neurol.* 268: 38-48, 1988.

MENDELSON, J. R. AND CYNADER, M. S. Sensitivity of cat primary auditory cortex (AI) neurons to the direction and rate of frequency modulation. *Brain Res.* 327: 331-335, 1985.

MENDELSON, J. R., SCHREINER, C. E., SUTTER, M. L. AND GRASSE, K. L. Functional topography of cat primary auditory cortex: responses to frequency-modulated sweeps. *Exp. Brain. Res.* 94: 65-87, 1993.

MERZENICH, M. M. AND BRUGGE, J. F. Representation of the cochlear partition on the superior temporal plane of the macaque monkey. *Brain Res.* 50: 275-296, 1973.

MERZENICH, M. M. AND SCHREINER, C. E. Mammalian Auditory Cortex - Some Comparative Observations. In: *The Evolutionary Biology of Hearing* edited by D. B. Webster, R. R. Fay and A. N. Popper. New York: Springer-Verlag, 1992, p. 673-685.

MOREL, A. AND IMIG, T. J. Thalamic projections to fields A, AI, P, and VP in the cat auditory cortex. *J. Comp. Neurol.* 265: 119-144, 1987.

PFINGST, B. E. AND O'CONNOR, T. A. Characteristics of neurons in auditory cortex of monkeys performing a simple auditory task. *J. Neurophysiol.* 45: 16-34, 1981.

PHILLIPS, D. P. AND IRVINE, D. R. F. Properties of single neurons in the anterior auditory field (AAF) of cat cerebral cortex. *Brain Res.* 248: 237-244, 1982.

PHILLIPS, D. P., JUDGE, P. W. AND KELLY, J. B. Primary auditory cortex in the ferret (*Mustela putorius*): neural response properties and topographic organization. *Brain Res.* 443: 281-294, 1988.

PHILLIPS, D. P., ORMAND, S. S., MUSICANT, A. D. AND WILSON, G. F. Neurons in the cat's primary auditory cortex distinguished by their responses to tones and wide-spectrum noise. *Hearing Res.* 18: 73-86, 1985.

REALE, R. A. AND IMIG, T. J. Tonotopic organization in auditory cortex of the cat. *J. Comp. Neurol.* 192: 265-291, 1980.

REDIES, H., SIEBEN, U. AND CREUTZFELDT, O. D. Functional subdivisions in the auditory cortex of the guinea pig. *J. Comp. Neurol.* 282: 473-488, 1989.

SCHREINER, C. E. AND MENDELSON, J. R. Functional topography of cat primary auditory cortex: distribution of integrated excitation. *J. Neurophysiol.* 64: 1442-1459, 1990.

SCHREINER, C. E. AND SUTTER, M. L. Topography of excitatory bandwidth in cat primary auditory cortex: single-neuron versus multiple-neuron recordings. *J. Neurophysiol.* 68: 1487-1502, 1992.

SHAMMA, S. A., FLESHMAN, J. W., WISER, P. R. AND VERSNEL, H. Organization of response areas in ferret primary auditory cortex. *J. Neurophys.* 69: 367 - 383, 1993.

SHAMMA, S. A., VERSNEL, H. AND KOWALSKI, N. Ripple analysis in ferret primary auditory cortex. I. Response characteristics of single units to sinusoidally rippled spectra. Institute for Systems Research, Technical Report: T.R. 94-20, 1994.

SUGA, N. Functional properties of auditory neurones inthe cortex of echo-locating bats. *J. Physiol. (Lond.).* 181: 671-700, 1965.

TOROS-MOREL, A., F., D. R. AND ROUILLER, E. Coding properties of the different nuclei of the cat's medial geniculate body. In: *Neuronal Mechanisms of Hearing* edited by J. Syka and L. Aitkin. New York: Plenum Publishing Corporation, 1981, p. 239-243.

TUNTURI, A. R. Frequency arrangement in anterior ectosylvian auditory cortex of dog. *Am. J. Physiol.* 203: 185-193, 1962.

VERSNEL, H., KOWALSKI, N. AND SHAMMA, S. A. Ripple analysis in ferret primary auditory cortex. II. Topographic and columnar distribution of ripple response parameters. Institute for Systems Research, Technical Report: T.R. 94-21, 1994.

VERSNEL, H. AND NELKEN, E. Comparison of responses to linear and logarithmic frequency modulated tonal stimuli in primary auditory cortex. *Assoc. Res. Otolaryngol. Abstr.* 17: 23, 1994.

WANG, K. AND SHAMMA, S. A. Self-normalization and noise robustness in auditory representations. *IEEE Trans. Audio. Speech. Proc.* 2: (in press), 1994.

WINER, J. A. The functional architecture of the medial geniculate body and the primary auditory cortex. In: *The Mammalian Auditory Pathway: Neuroanatomy* edited by D. B. Webster, A. N. Popper and R. R. Fay. New York: Springer-Verlag, 1992, p. 222-409.

ZEKI, S. AND SHIPP, S. The functional logic of cortical connections. *Nature.* 335: 311-317, 1988.

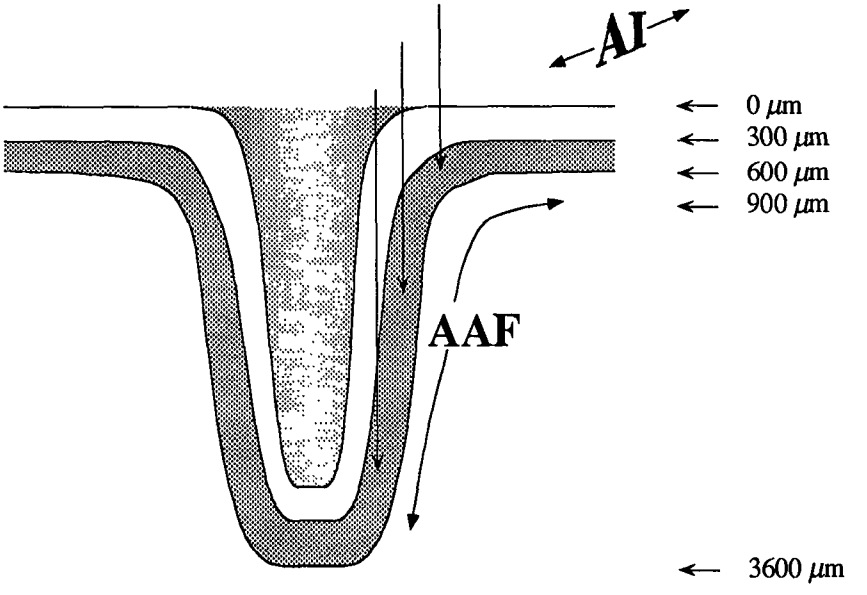

Figure 1. Schematic showing electrode penetrations into AAF along the ectosylvian sulcus. High frequencies are located at the top of the penetration and low frequencies toward the bottom.

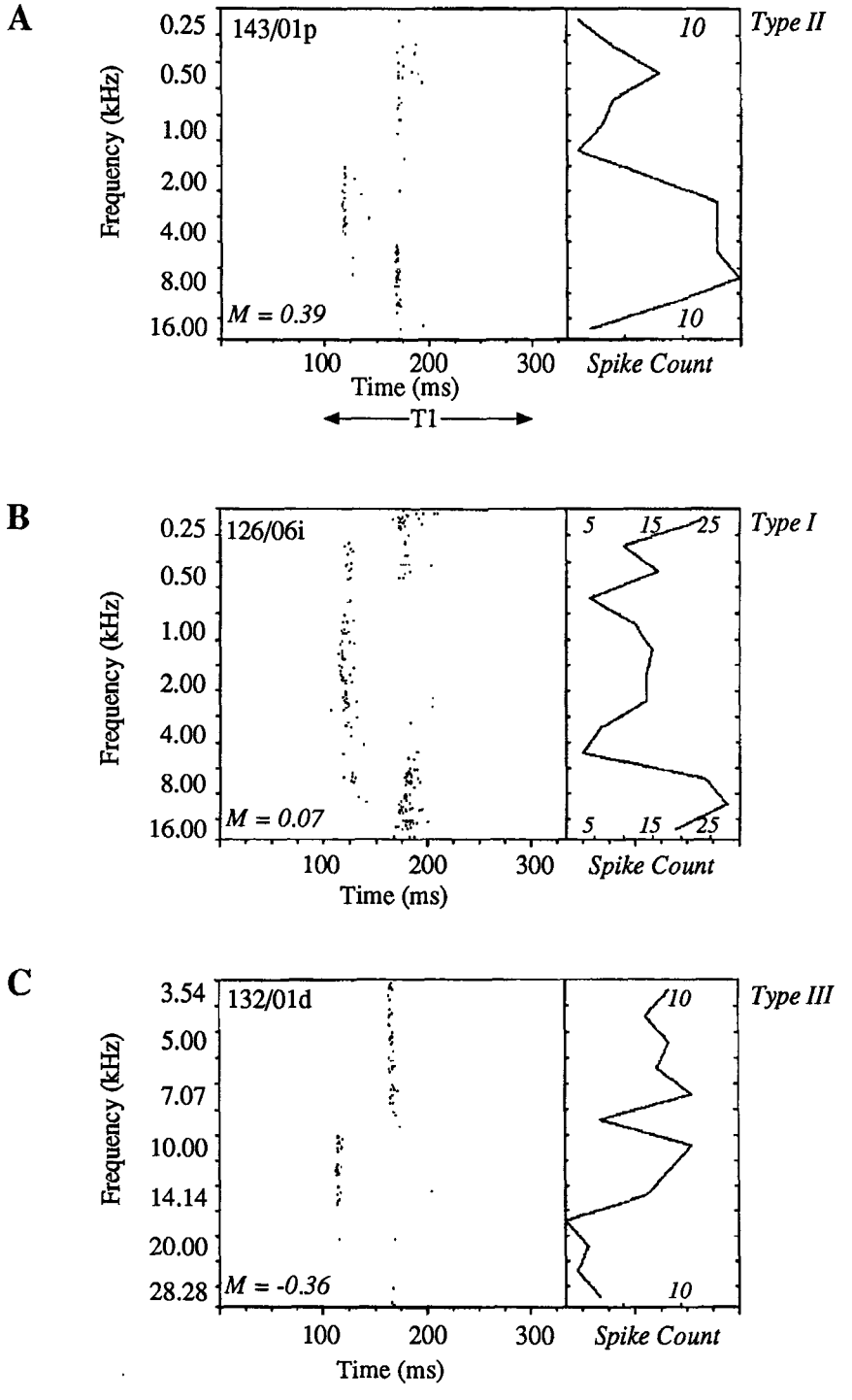

Figure 2. Raster plots describing three types of responses to a two-tone test. T1 and T2 tone durations are indicated. The time window for measuring the response is between 110 and 200 ms. The curve displayed on its side is the total spike count at each frequency over the time window. The M index describes the asymmetry of the spike count curve about the best frequency. M indices of type I responses are close to zero and indicate a symmetric response curve, whereas M indices of types II and III correspond to asymmetric response curves. In all examples, T1 and T2 are presented at 65 dB SPL, and 20 repetitions are made at each T1 frequency. A: Example of response classified as Type II. Total spike count decreases below the best frequency ~4 kHz. T2 is fixed at 4 kHz. B: In this example of a Type I response, the response curve is even about BF ~2 kHz. T2 is set to 2 kHz. C: Example of response classified as Type III. The response curve decreases above BF ~10 kHz. T2 is fixed at 10 kHz.

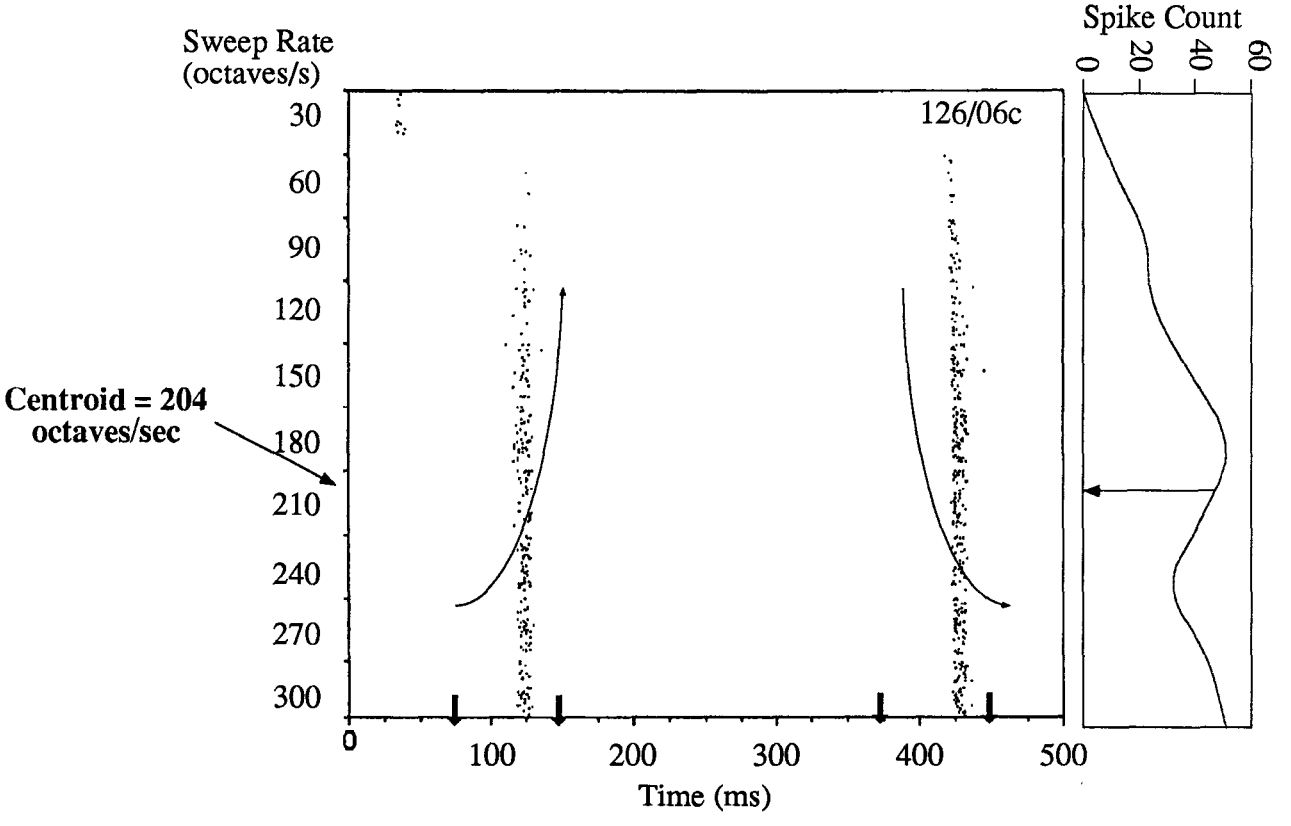

Figure 3. Raster plot of a unit's response to FM stimuli. Each FM stimuli consists of an upsweep first, then the down sweep, for a range of sweep rates. The stimuli are designed such that the BF of the unit is traversed at 100 ms upsweep and 400 ms down sweep. The sweep begins 1 or 1.5 octaves below BF and extends to 1 or 1.5 octaves above BF for the upsweep and vice-versa for the down sweep. The C index and centroid are measured from this paradigm. The time windows of measurement are indicated by the downward arrows. The curve on its side represents the spike count curve for the upsweep or down sweep, whichever resulted in the larger total number of spikes. The centroid of the curve is used to locate the preferred rate of the unit by using the curve to weight each rate, then taking the weighted average.

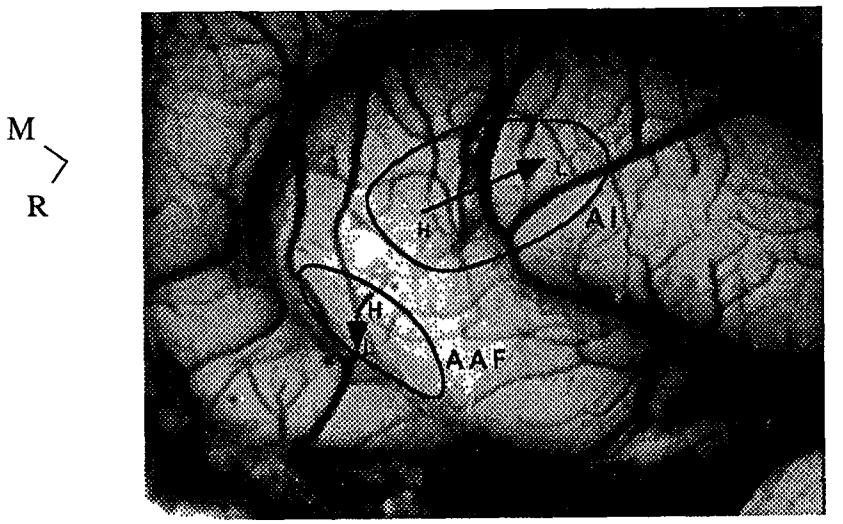

Figure 4. Picture of the ectosylvian gyrus and part of the suprasylvian sulcus, showing where AI and AAF are located respectively to each other. The length of the arrow showing the tonotopicity of AI corresponds to a length of approximately 3 mm.

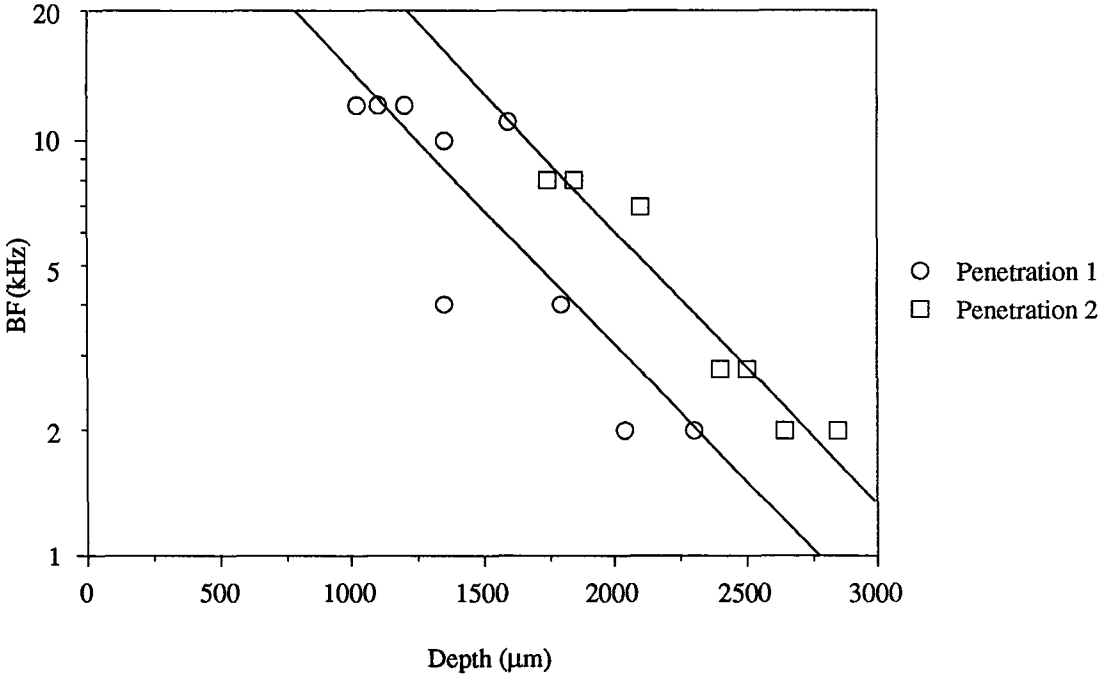

Figure 5. Examples of the decrease in BF with increasing depth along AAF, down the suprasylvian sulcus. Penetrations 1 and 2 are from experiments 136 and 143 respectively.

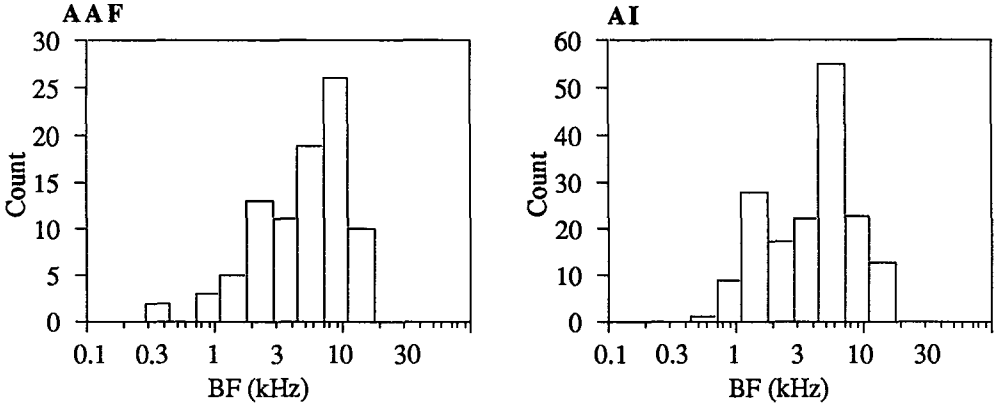

Figure 6. Distribution of BFs in AAF and AI.

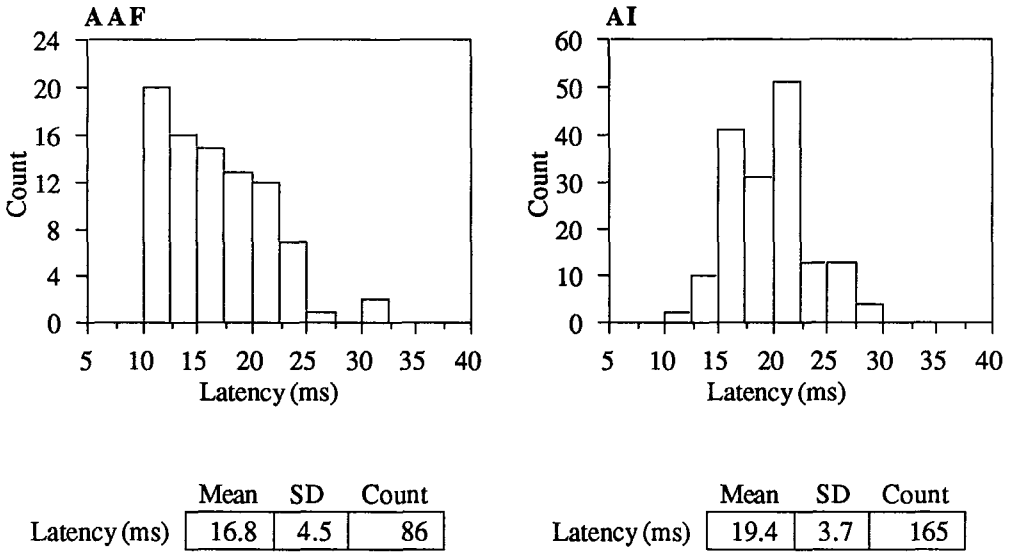

	Mean	SD	Count
Latency (ms)	16.8	4.5	86

	Mean	SD	Count
Latency (ms)	19.4	3.7	165

Figure 7. Distribution of latencies to tone onset in AAF and AI. The mean latency of an AAF unit (16.5 ms) is significantly shorter than the mean latency found in AI (19.4 ms) ($P<0.05$).

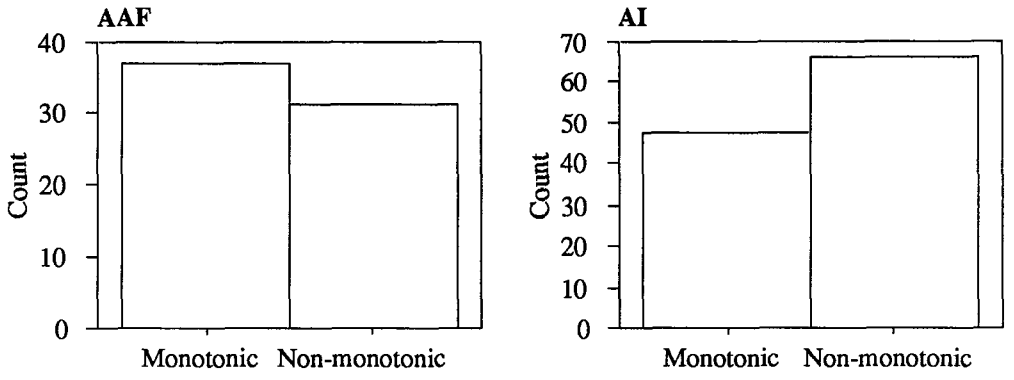

Figure 8. Distribution of monotonic units and non-monotonic units in AAF and AI. Both fields have similar proportions of non-monotonic units (45% non-monotonic in AAF, 58% non-monotonic in AI).

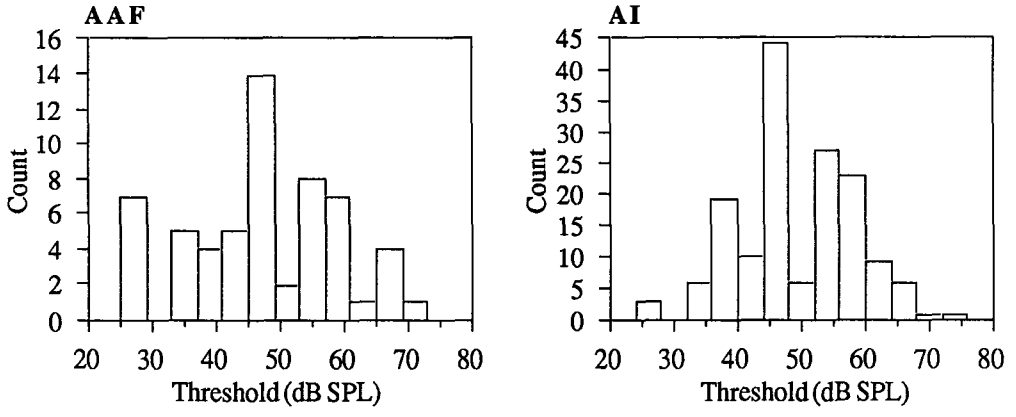

	Mean	SD	Count
Threshold (dB SPL)	47.0	11.8	58

	Mean	SD	Count
Threshold (dB SPL)	48.8	9.1	155

Figure 9. Distribution of thresholds at BF in AAF and AI. Mean thresholds are not statistically different (P>0.05) between AAF and AI (47.0 dB in AAF, 48.8 dB in AI).

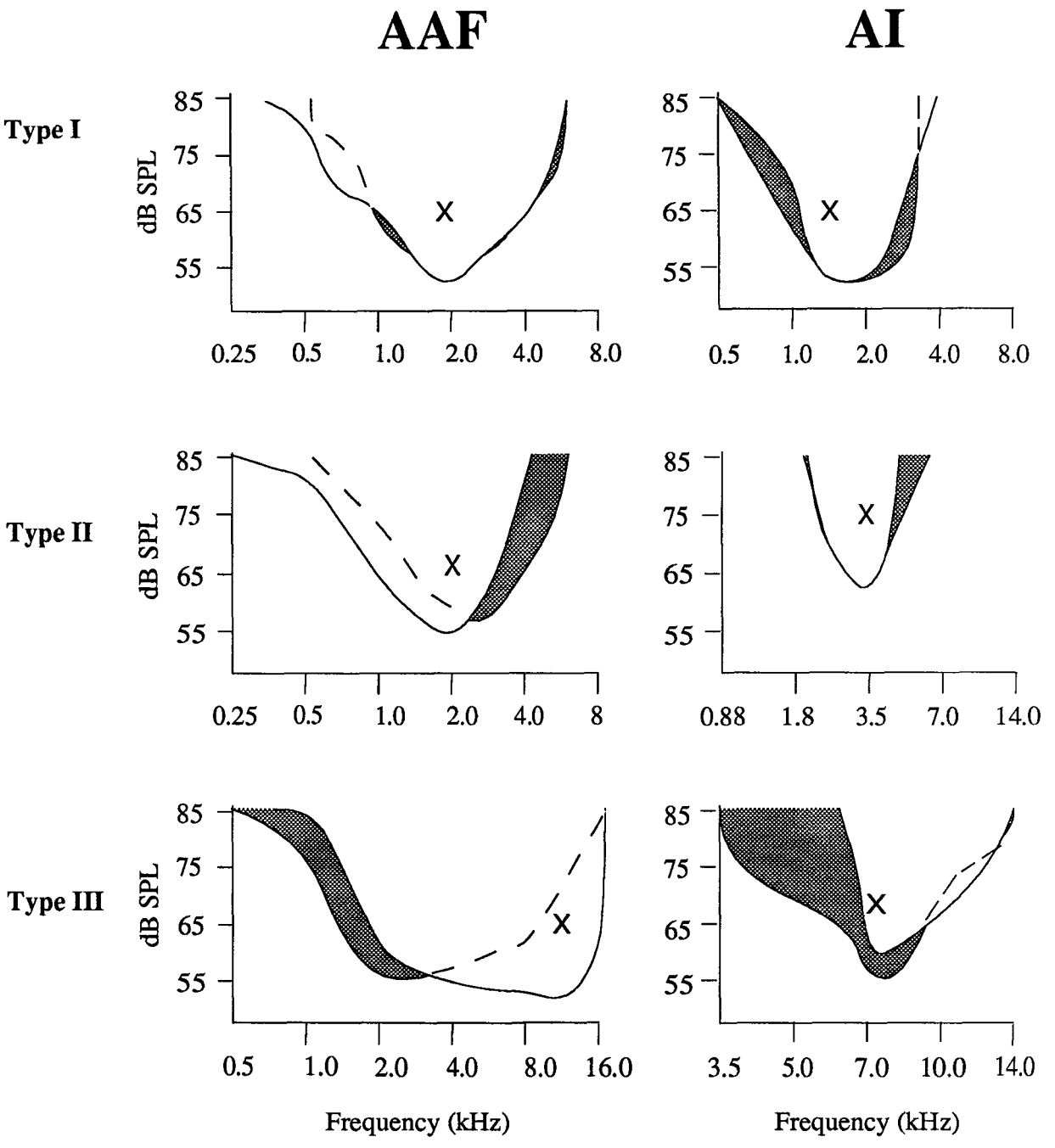

Figure 10. Examples of response areas of six units from AAF and AI. Units in the AAF have broader excitatory areas than those in AI, but have similar response area asymmetries. Variation of response area asymmetry (three types) is found in both AI and AAF. 'x' marks the best frequency. Shaded areas are inhibitory, white areas are excitatory.

A

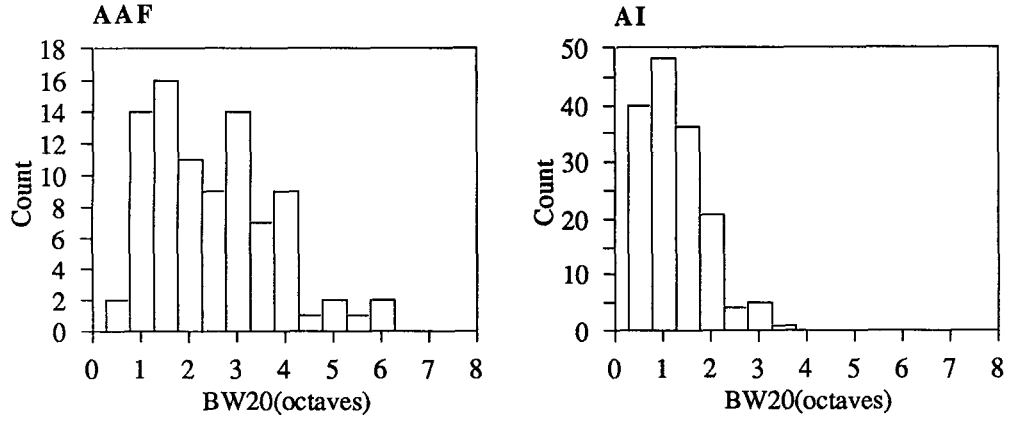

	Mean	SD	Count
BW20(octaves)	2.48	1.28	88

	Mean	SD	Count
BW20(octaves)	1.26	0.66	155

B

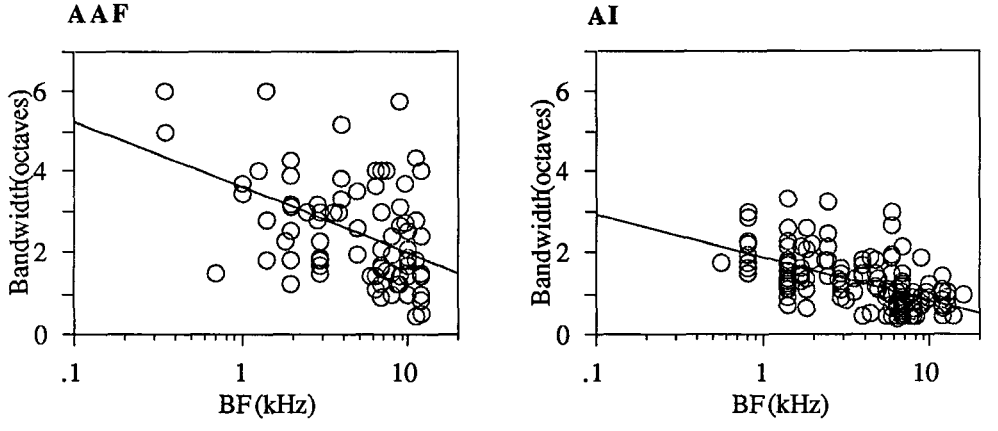

	R	P	Count
BW20 vs. BF	0.47	<0.0001	88

	R	P	Count
BW20 vs. BF	0.51	<0.0001	155

Figure 11. The distribution of BW20 in AAF and AI is shown in Fig. 11A. The mean BW20 is much wider in AAF (2.5) than in AI (1.3). The difference is statistically significant ($P<0.05$). Fig. 11B shows that a similar relationship between BW20 and BF is found in both AAF and AI. The equation for the AAF regression line is: BW20 (oct) = 3.6 - 1.6*log(BF). The equation for the AI regression line is: BW20 (oct) = 1.9 - 1.0*log(BF). In both fields, there is a systematic decrease in BW20 as BF increases.

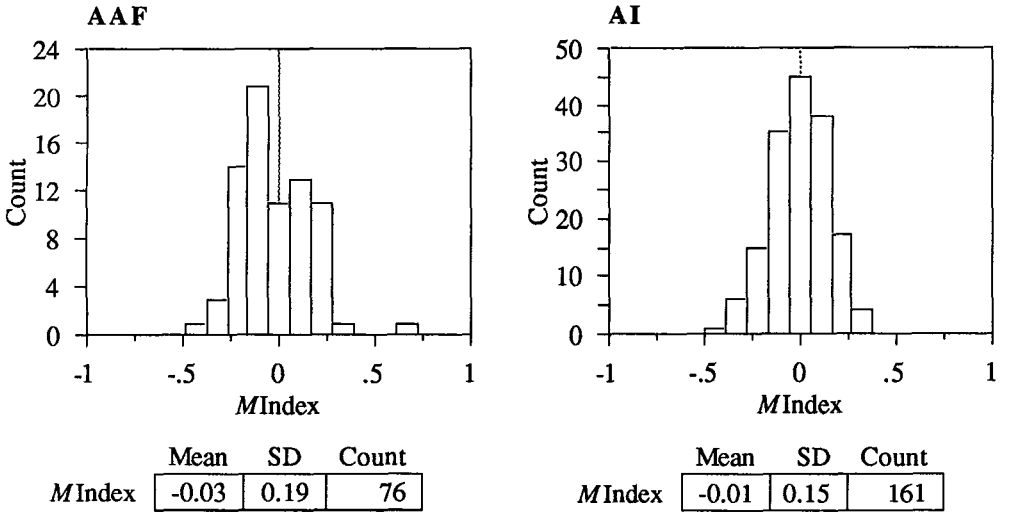

	Mean	SD	Count
M Index	-0.03	0.19	76

	Mean	SD	Count
M Index	-0.01	0.15	161

Figure 12. Distribution of M indices in AAF and AI. An M index value between ± 0.08 corresponds to a unit with type I response area. M index values less than -0.08 and greater than +0.08 correspond to response area types II and III, respectively. AAF and AI have similar distributions of M indices.

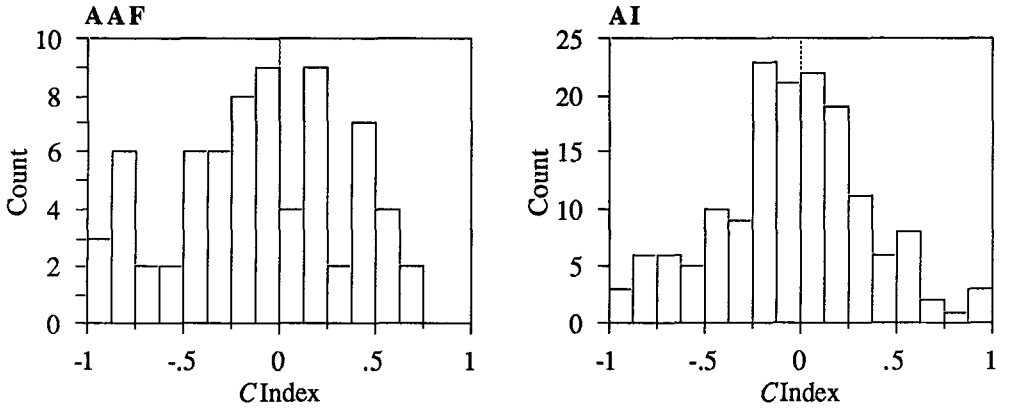

	Mean	SD	Count
C Index	-0.11	0.44	70

	Mean	SD	Count
C Index	-0.05	0.39	155

Figure 13. Distribution of C indices in AAF and AI. AAF and AI have similar distributions of C indices.

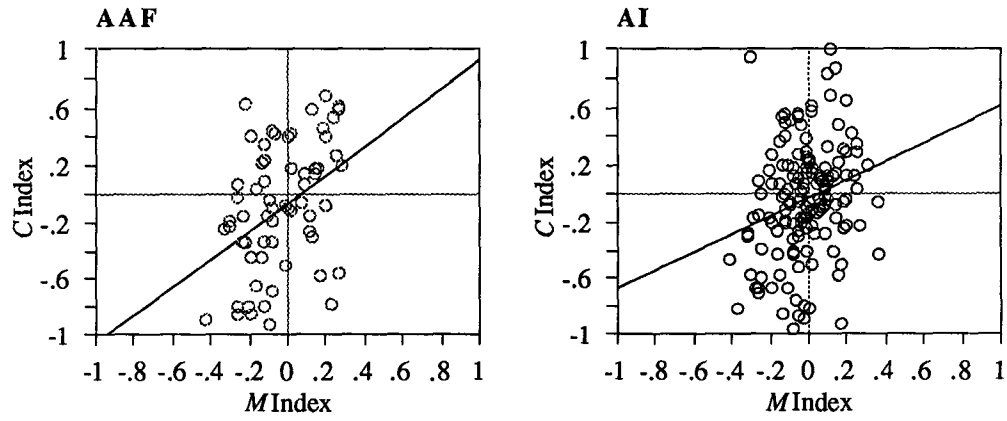

	R	P	Count
M vs. *C*	0.39	0.001	64

	R	P	Count
M vs. *C*	0.25	0.002	150

Figure 14. Correlation between asymmetry indices C and M is significant in AAF and AI ($P < 0.05$). Data are obtained from 64 units in 7 animals from AAF and 150 units from 17 animals in AI.

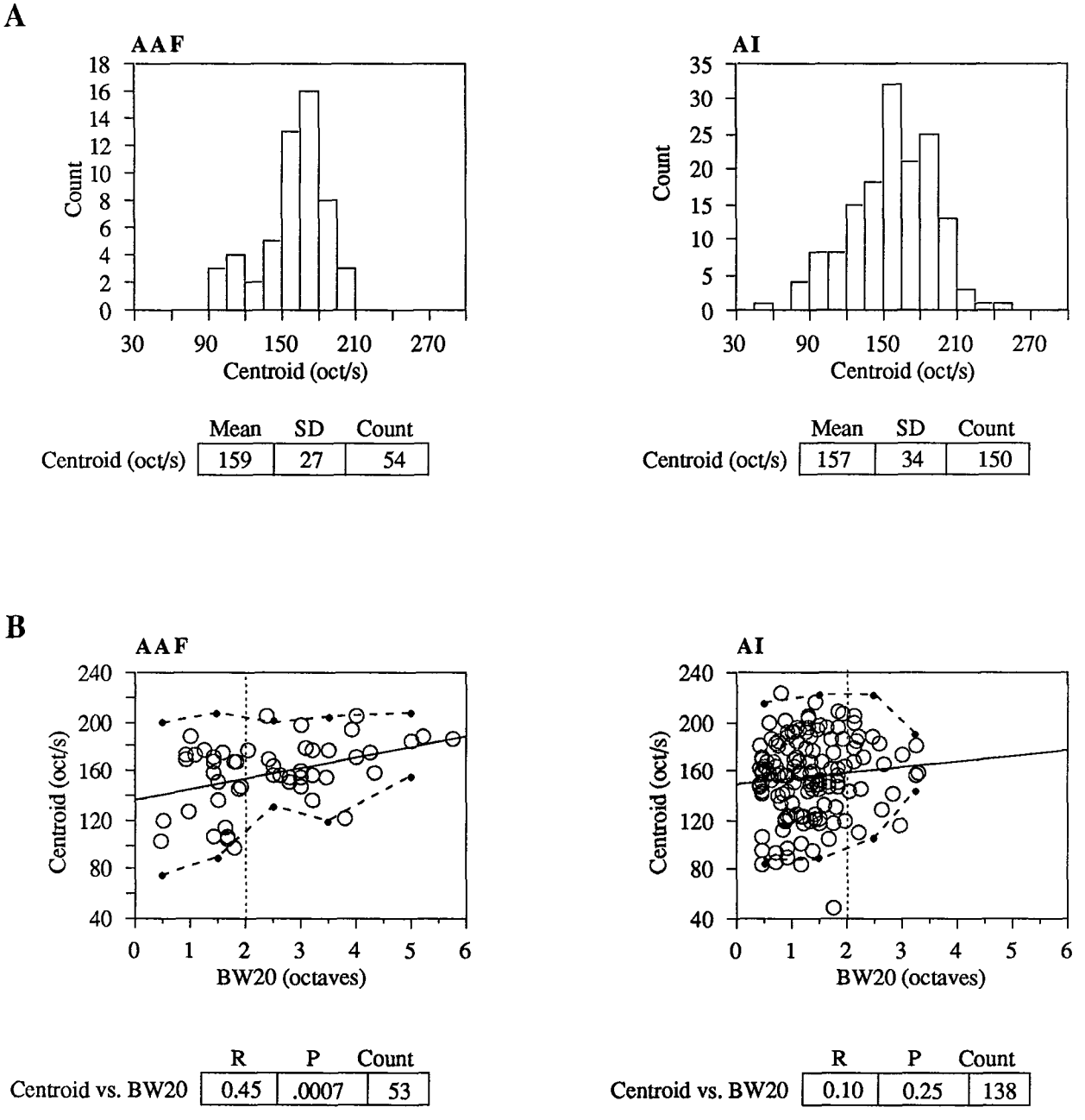

	Mean	SD	Count
Centroid (oct/s)	159	27	54

	Mean	SD	Count
Centroid (oct/s)	157	34	150

	R	P	Count
Centroid vs. BW20	0.45	.0007	53

	R	P	Count
Centroid vs. BW20	0.10	0.25	138

Figure 15. Centroids of FM rate in AAF and AI. Fig. 15A shows the distribution of centroids in each field. The mean centroid did not differ significantly between AAF and AI, but the standard deviation of the AI centroid population was significantly larger than in AAF. Fig. 15B shows that the linear correlation between centroid and BW20 is significant in AAF ($P<0.05$) and not in AI ($P>0.05$). The relationship between centroid and BW20 in both fields can be described by the variance of centroids with BW20. The mean and SD of centroid populations corresponding to BW20 ranges 0-1, 1-2, 2-3, 3-4 (and 4+ in AAF) octaves were calculated. The bullet points (•) indicate ±2SD from the mean of centroids in each BW20 range. The dashed lines connect the • points and show the trends in centroid variance as BW20 increases. The dotted line indicates where BW20=2.0 octaves. For BW20 values larger than 2.0 octaves, the SD of the centroid population is 27 in AI and 20 in AAF, and for BW20 smaller than 2.0, the SD of each population is 33 in AI and 30 in AAF.

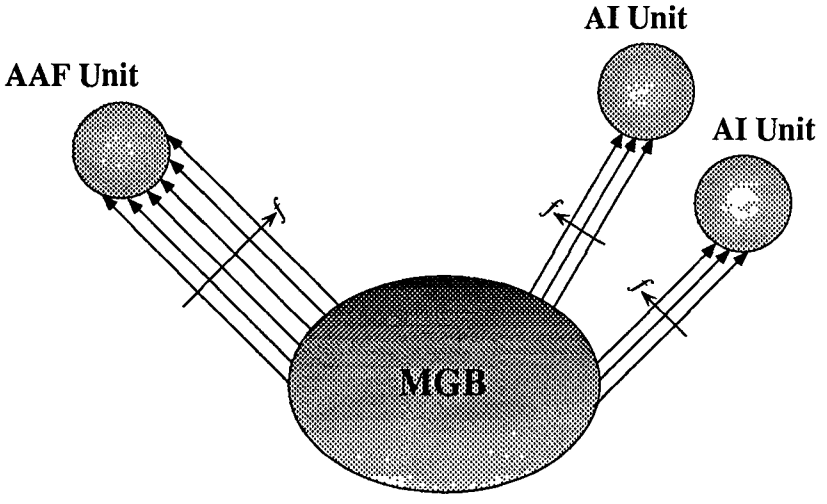

Figure 16. Schematic of hypothesized afferent connections from MGB to AAF and AI. AAF may receive inputs that converge on a physically smaller area, thus generating larger response areas. The AAF and AI units are indicated, with one AAF unit receiving twice as many inputs as a unit in AI. The smaller arrows indicate that the inputs frequencies vary in an orderly manner. The MGB oval represents the origin of the thalamocortical afferents. The exact location of projections to AAF in the ferret are unknown.